Magnetic properties of a quantum spin ladder in proximity to the isotropic limit

S. A. Zvyagin,[1,*] A. N. Ponomaryov,[1,†] M. Ozerov,[1,‡] E. Schulze,[1,2] Y. Skourski,[1] R. Beyer,[1] T. Reimann,[1] L. I. Zviagina,[1] E. L. Green,[1,‡] J. Wosnitza,[1,2] I. Sheikin,[3] P. Bouillot,[4] T. Giamarchi,[4] J. L. Wikara,[5] M. M. Turnbull,[6] and C. P. Landee[7,§]

[1]*Dresden High Magnetic Field Laboratory (HLD-EMFL) and Würzburg-Dresden Cluster of Excellence ct.qmat, Helmholtz-Zentrum Dresden-Rossendorf, D-01328 Dresden, Germany*

[2]*Institut für Festkörper- und Materialphysik, TU Dresden, D-01062 Dresden, Germany*

[3]*Laboratoire National des Champs Magnétiques Intenses (LNCMI-EMFL), CNRS, UGA, F-38042 Grenoble, France*

[4]*Department of Quantum Matter Physics, University of Geneva, CH-1211 Geneva, Switzerland*

[5]*School of Physical and Chemical Sciences, University of Canterbury, Christchurch 8041, New Zealand*

[6]*Carlson School of Chemistry and Biochemistry, Clark University, Worcester, Massachusetts 01060, USA*

[7]*Department of Physics and Carlson School of Chemistry, Clark University, Worcester, Massachusetts 01060, USA*

(Received 16 February 2021; revised 27 April 2021; accepted 28 April 2021; published 18 May 2021)

We report on the synthesis, crystal structure, magnetic, thermodynamic, and electron-spin-resonance properties of the coordination complex $[Cu_2(pz)_3(4\text{-}HOpy)_4](ClO_4)_4$ (pz=pyrazine; 4-HOpy=4-hydroxypyridine). This material is identified as a spin-1/2 Heisenberg ladder system with exchange-coupling parameters $J_{rung}/k_B = 12.1(1)$ K and $J_{leg}/k_B = 10.5(3)$ K [$J_{rung}/J_{leg} = 1.15(4)$]. For single crystals our measurements revealed two critical fields, $\mu_0 H_{c1} = 4.63(5)$ T and $\mu_0 H_{c2} = 22.78(5)$ T (for $H \parallel a^*$), separating the gapped spin-liquid, gapless Tomonaga-Luttinger-liquid, and fully spin-polarized phase. No signature of a field-induced transition into a magnetically ordered phase was found at temperatures down to 450 mK. The material bridges an important gap by providing an excellent physical realization of an almost isotropic spin-1/2 strong-rung Heisenberg ladder system with modest exchange-coupling energy and critical-field scales.

DOI: 10.1103/PhysRevB.103.205131

I. INTRODUCTION

Spin-1/2 Heisenberg antiferromagnetic (AF) ladders continue to attract considerable attention, providing an excellent ground for testing various concepts of materials science and quantum physics [1,2]. Apart from their possible relevance to high-temperature superconductivity [1,3,4], the interest in these systems is motivated by their unusual ground-state properties and spin dynamics. In zero magnetic field, the ground state of a two-leg spin-1/2 AF ladder is a nonmagnetic singlet, separated from the first excited triplet by an energy gap. At a first critical field, H_{c1}, the gap closes and the ladder undergoes a transition into a gapless phase with a magnetic ground state. In this phase, the system can be mapped onto a network of interacting bosons with the density of states controllable by the applied magnetic field. At low-enough temperatures, when three-dimensional (3D) correlations are relevant, the system undergoes a transition into a 3D ordered state (a process that is often referred to as magnon Bose-Einstein condensation [5,6]). Above the ordering temperature, short-range correlations are still relevant; the field-induced phase can be regarded as a Tomonaga-Luttinger liquid (TLL), with the spin-spin correlation function decaying as a power law and spinons as elementary magnetic excitations. Recently, the TLL behavior in this intermediate phase of a spin ladder has been studied theoretically and experimentally in detail [7–9]. At a second critical field, H_{c2}, the system undergoes a transition into a classical spin-polarized magnetically saturated phase.

The Hamiltonian for a two-leg spin-1/2 Heisenberg AF ladder can be written as

$$\mathcal{H} = J_{leg} \sum_{\langle l,j \rangle} \mathbf{S}_{l,j} \cdot \mathbf{S}_{l+1,j} + J_{rung} \sum_{\langle l \rangle} \mathbf{S}_{l,1} \cdot \mathbf{S}_{l,2} - g\mu_B H \sum_{l,j} S^z_{l,j} + \mathcal{H}_\delta, \quad (1)$$

where J_{leg} and J_{rung} are exchange-coupling constants along the legs and rungs, respectively, $\mathbf{S}_{l,j}$ are the spin operators on site l of the ladder leg ($j = 1, 2$), and $g\mu_B H$ is the Zeeman term (g is the g factor, μ_B is the Bohr magneton, and H is the applied magnetic field). The fourth term represents various possible, usually small, anisotropic contributions.

In the limit $\gamma = J_{rung}/J_{leg} \to \infty$, a two-leg ladder can be regarded as a network of isolated spin dimers. For $\gamma = 0$ the gap vanishes and the system is equivalent to a spin-1/2 Heisenberg AF chain. It would be interesting to experimentally study the evolution between the strong-rung ($\gamma > 1$) and

*Corresponding author: s.zvyagin@hzdr.de

†Present address: Institute of Radiation Physics, Helmholtz-Zentrum Dresden-Rossendorf, 01328 Dresden, Germany.

‡Present address: National High Magnetic Field Laboratory, Florida State University, Tallahassee, FL 32310, USA.

§Corresponding author: clandee@clarku.edu

 ©2021 American Physical Society

strong-leg ($\gamma < 1$) phases, in particular in the vicinity of the critical ($\gamma \sim 1$) regime [10–13].

Recent progress in coordination chemistry made it possible to synthesize new materials with variable γ and accessible critical fields (for a review, see, e.g., Ref. [14]), allowing one to systematically study the magnetic properties of quantum spin ladders across different regions of their phase diagrams. Among others, the strong-leg ladder compound DIMPY [chemical formula $(C_7H_{10}N)_2CuBr_4$; $\gamma = 0.58$] [15–24] and strong-rung ladder material BPCB [chemical formula $(C_5H_{12}N)_2CuBr_4$; $\gamma \approx 3.6$] [7–9,25–30] are the most intensively studied. The exchange-coupling ratio of another strong-rung ladder compound, Cu(quinoxoline)Cl_2, $\gamma = 1.58$, is much closer to unity [31]. The case of an isotropic ladder ($\gamma \sim 1$) has been less studied, presented only by the compound (5-NAP)$_2CuBr_4 \cdot H_2O$ with $\gamma = 1.04$ [32] (currently available only in the polycrystalline form).

Here, we report on the synthesis, crystal structure, magnetic, thermodynamic, and electron-spin-resonance properties of another coordination complex compound, copper pyrazine pyridone perchlorate (hereafter CPPP), with the chemical formula $[Cu_2(pz)_3(4\text{-HOpy})_4](ClO_4)_4$ (pz=pyrazine; 4-HOpy=4-hydroxypyridine). This material is available in single-crystal form and characterized by $\gamma = 1.15$, bridging an important gap between Cu(quinox)Cl and (5-NAP)$_2CuBr_4 \cdot H_2O$ and providing an excellent realization of a two-leg spin-1/2 strong-rung ladder in close proximity to the isotropic limit with modest exchange-coupling parameters and critical fields.

II. EXPERIMENTAL DETAILS

X-ray data collection for CPPP was carried out on an Oxford Gemini diffractometer employing graphite-monochromated Mo $K\alpha$ radiation, using ω scans. Data collection and reduction were done using CRYSALISPRO [33], while absorption corrections were made analytically employing the method of Clark and Reid within the CRYSALISPRO software. The structure solution was carried out using SHELXS-97 [34], while refinements were performed using SHELXL-2018 [35]. All nonhydrogen atoms were refined using anisotropic thermal parameters. All hydrogen atoms were refined with fixed isotropic thermal parameters. Those bonded to carbon atoms were inserted geometrically and refined with a riding model, while those bonded to N atoms were located in the lattice and their positions refined. For ESR experiments single crystals were oriented at room temperature by using an INEL Equinox 3000 Laue diffractometer.

Infrared (IR) spectra were obtained with a Perkin Elmer Spectrum 100 Fourier transform infrared (FT-IR) spectrometer. Elemental analyses were performed at the Marine Science Institute, University of California-Santa Barbara, CA, USA. Magnetic susceptibility (M/B, where M is the magnetic moment) was measured in Clark University using a magnetic properties measurement system (MPMS-XL) superconducting quantum interference device (SQUID) magnetometer (Quantum Design) at temperatures down to 1.8 K.

Torque magnetometry was performed at the LNCMI-Grenoble, France, in magnetic fields up to 32 T, using a capacitive beam cantilever mounted on a rotator and placed in a top-loading ^{3}He / ^{4}He dilution refrigerator. High-field magnetization was measured at the HLD, Dresden, Germany, using a pulsed magnet with a rise time of 7 ms and a total pulse duration of 25 ms. The magnetization was obtained by integrating the voltage induced in a compensated coil system surrounding the sample [36].

The specific heat was measured at temperatures down to ca. 0.5 K in magnetic fields up to 15 T using a superconducting

TABLE I. Crystal data and structure refinement.

Empirical formula	$C_{16}H_{16}Cl_2CuN_5O_{10}$
Formula weight	572.78 g/mol
Data collection temperature	123(2) K
Crystal system	Monoclinic
Space group	$P2_1/c$
Unit-cell dimensions	$a = 18.9263(13)$ Å
	$b = 6.9072(2)$ Å
	$c = 16.8169(6)$ Å
	$\alpha = 90^\circ$
	$\beta = 105.031(5)^\circ$
	$\gamma = 90^\circ$
Volume	2123.22(18) Å^3
Z	4
Density (calculated)	1.792 Mg/m^3
Absorption coefficient	1.348 mm^{-1}
$F(000)$	1160
Crystal size	$0.66 \times 0.43 \times 0.16$ mm^3
Theta range	3.153°-41.046°
Index ranges	$-34 \leqslant h \leqslant 34$
	$-12 \leqslant k \leqslant 12$
	$-23 \leqslant l \leqslant 3$
Independent reflections	14392
Data/restraints/parameters	14392/0/314
Goodness-of-fit on F^2	1.024
Final R indices [$I > 2\sigma(I)$]	$R1 = 0.0521$, $wR2 = 0.1281$
R indices (all data)	$R1 = 0.0903$, $wR2 = 0.1386$
Largest diff. peak and hole	1.331 and -1.374 e Å^{-3}

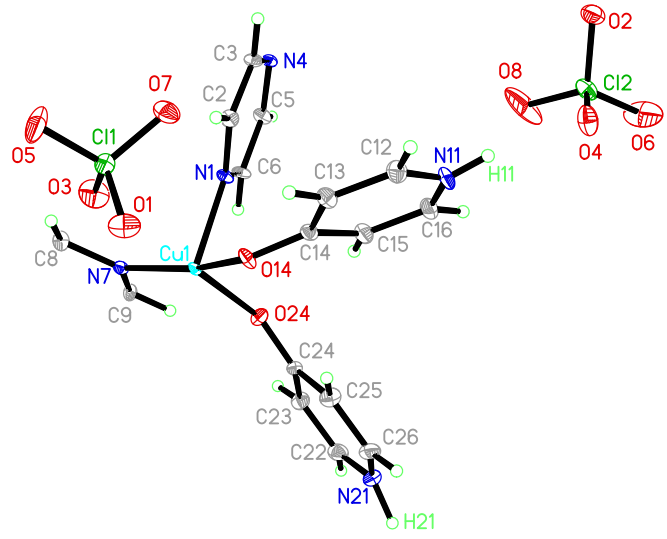

FIG. 1. A thermal ellipsoid plot of the asymmetric unit of CPPP. Hydrogen atoms are shown as spheres of arbitrary size. Only those hydrogen atoms whose positions were refined are labeled.

TABLE II. Selected bond lengths (Å) and angles (deg). Symmetry transformations used to generate equivalent atoms: #1 $x, y-1, z$.

Cu1-O14	1.9163(17)	Cu1-N7	2.0309(19)
Cu1-N4#1	2.0603(18)	Cu1-N1	2.0631(18)
Cu1-O24	2.1548(18)	Cu1O3	2.990(3)
O14-Cu1-N7	162.28(8)	O14-Cu1-N4#1	88.03(7)
N7-Cu1-N4#1	88.61(8)	O14-Cu1-N1	92.33(7)
N7-Cu1-N1	89.24(8)	N4#1-Cu1-N1	173.98(8)
O14-Cu1-O24	106.55(7)	N7-Cu1-O24	91.06(7)
N4#1-Cu1-O24	94.55(7)	N1-Cu1-O24	91.10(7)

magnet with a HelioxVL ^{3}He insert (Oxford Instruments). The heat capacity was determined from the time dependence of the temperature relaxation as described in Ref. [37].

Electron spin resonance (ESR) measurements were performed using a Bruker ELEXSYS E500 spectrometer at a frequency of 9.4 GHz at temperatures down to 2 K. The spectrometer is equipped with a continuous flow cryostat (Oxford Instruments). To estimate ESR parameters (the full width at half maximum, resonance field position, and integrated intensity) the spectra were fit using the Lorentzian line-shape function.

The density matrix renormalization group (DMRG) calculations are done by a finite DMRG code with conserved quantum number S^z, similar to the one used and described in Ref. [8]. The system consists of ladders of 200 rungs, and 256 states were conserved in the Schmidt decomposition.

III. SYNTHESIS

To grow crystals, $Cu(ClO_4)_2 \cdot 6H_2O$ (1.824 g, 4.9 mmol), pyrazine (802 mg, 10.0 mmol), and 4-hydroxypyridine (957 mg, 10.1 mmol) were each dissolved in 2 ml of MeOH. The pz solution was then rinsed into the stirred pyridone solution with an additional 2 ml MeOH. This combined solution was added slowly to the stirred copper solution. The initial medium-blue solution rapidly darkened and a precipitate appeared before a third of the organic solution was added. Once the solutions were totally combined, 2 ml of MeOH was added and stirred for another 45 min. The mixture was filtered through a fine frit, rinsed with 2 ml MeOH, then dried under vacuum for 90 min. The light-blue product was dried to a constant weight of 1.866 mg. The light-blue filtrate was transferred to a 50-ml beaker, partially covered, and set aside. Within 2 weeks, small (with the size up to $3 \times 3 \times 0.5$ mm^3) flat blue-green crystals appeared on the sides and bottom of the beaker. They were collected, rinsed with MeOH, and dried under vacuum to a constant weight of 253 mg. The yield (based on copper)=8.8%. The IR (cm^{-1}) was as follows: 3318 (w), 1637 (m), 1581 (m), 1540 (m), 1518 (s), 1429 (m), 1383 (m), 1192 (m), 1155 (m), 1117 (w, sh), 1076 (w, sh), 1065 (s), 1040 (w, sh), 997 (m), 928 (w), 862 (w), 827 (m), 754 (m), 620 (s), 572 (w) (here, the intensities are indicated as s=strong, m=medium, w=weak, and sh=shoulder). The combustion analysis showed the following: Found (%, duplicate trials): C 33.6, 33.5; H 2.83, 2,61; N 12.2; 12.2. Calculated (%): C 33.6; H 2.80; N 12.2. The immediate light-blue precipitate corresponds to the pyrazine-bridged hydrated copper chain with the formula $[Cu(pz)(H_2O)_2(4\text{-}OHpy)_2](ClO_4)_2$.

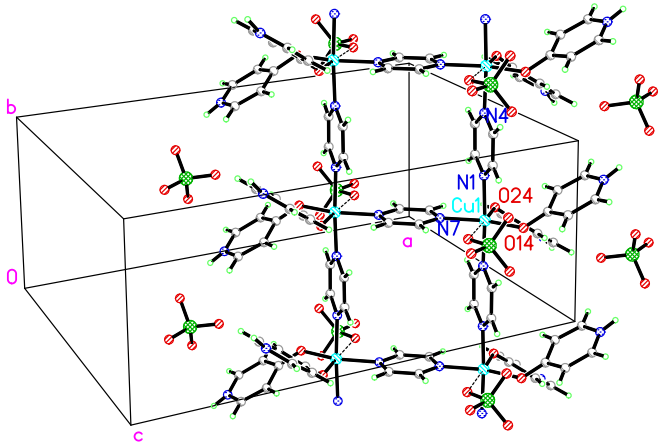

FIG. 2. The ladder structure of CPPP [light blue (Cu), black (C), red (O), green (Cl), turquoise (H)]. The ladder extends along the b axis.

IV. STRUCTURE ANALYSIS

The crystal data and structure refinement of CPPP, as obtained by our x-ray structural studies, are summarized in Table I. The asymmetric unit (shown in Fig. 1) comprises one Cu(II) ion, 1.5 pyrazine molecules, two 4(1H)-pyridone molecules, and two perchlorate anions. Each copper ion exists in a significantly distorted octahedral geometry (perhaps better described as $4+1+1$) with four short bonds to three N atoms from pyrazine ligands and the O atom from one pyridone (which constitute the equatorial plane), one slightly longer bond to the O atom of the second pyridone ligand, and a very long (~3 Å) contact to an oxygen (O3) of one of the perchlorate anions. The greatest deviation from octahedral geometry is the N7-Cu1-O14 bond angle [162.28(8)°]. Table II contains selected bond lengths and angles around the Cu(II) ion.

There are two crystallographically independent pyrazine ligands. One, the ring containing N1 and N4, forms bridges parallel to the b axis, linking Cu(II) ions in successive unit cells into chains with a 6.907 Å separation (the b-axis repeat unit). The second pyrazine ring (containing N7) sits athwart a crystallographic inversion center, hence only one-half of the ring is seen in the asymmetric unit (Fig. 1). This pyrazine ring links pairs of Cu(II) ions with a CuCu distance of 6.841 Å, slightly shorter than that through the N1 pyrazine ring. The combination of pyrazine bridges links the asymmetric units covalently into a ladder structure parallel to the b axis (Fig. 2).

The ladders are well isolated in the lattice. The packing structure of CPPP viewed parallel to the b axis is shown in Fig. 3. Successive ladders parallel to the a axis are offset by one-half unit cell (parallel to b) and separated by the interdigitated pyridone ligands with a minimum CuCu distance of 13.10 Å, while the closest CuCu distance between successive ladders in the c direction is 9.08 Å.

The lattice is stabilized by bifurcated hydrogen bonds between the pyridone N-H hydrogen atoms and oxygen atoms from the Cl2-perchlorate ion (Fig. 4). The hydrogen bonds

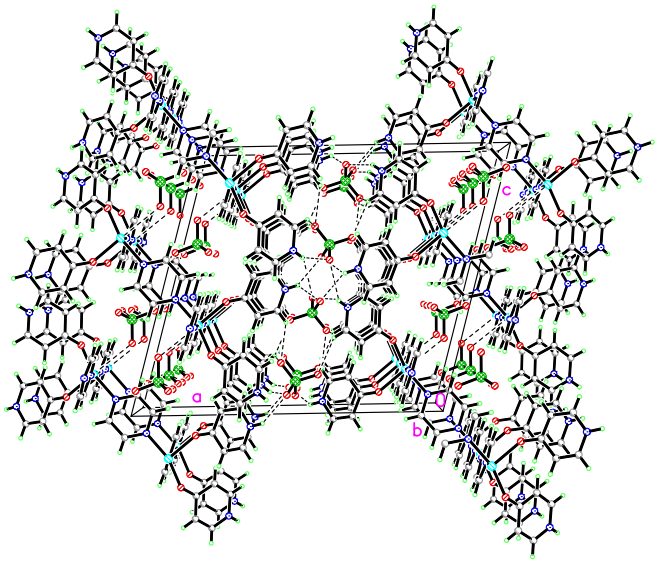

FIG. 3. The packing structure of CPPP viewed parallel to the b axis [a is horizontal; light blue (Cu), black (C), red (O), green (Cl), turquoise (H)]. Dashed lines represent hydrogen bonds.

(see Table III for details) result in unusually short O2O2 and O4O4 distances (2.90 and 2.83 Å, respectively).

V. MAGNETIC PROPERTIES

The magnetic susceptibility of a powder sample at a temperature of 1.5 K is shown in Fig. 5. The data display a rounded maximum near 9 K, characteristic of short-range correlations. The rapid descent towards zero at the lowest temperature (1.8 K) is indicative of a spin-singlet ground state. The solid red line through the data points in Fig. 5 corresponds to results of calculations [38], revealing $J_{\rm leg}/k_B = 10.5(3)$ K and $J_{\rm rung}/k_B = 12.1(1)$ K [$\gamma = 1.15(4)$] (which are very close to the parameters mentioned in Ref. [39]). Figure 6 shows pulsed-field magnetization data of a powder sample at a temperature of 1.5 K, indicating change of the magnetization behavior at about 4.5 and 23 T, which corresponds to transitions to the gapless TTL and magnetically saturated phase, respectively.

In order to accurately determine the critical fields we performed high-field low-temperature torque-magnetometry

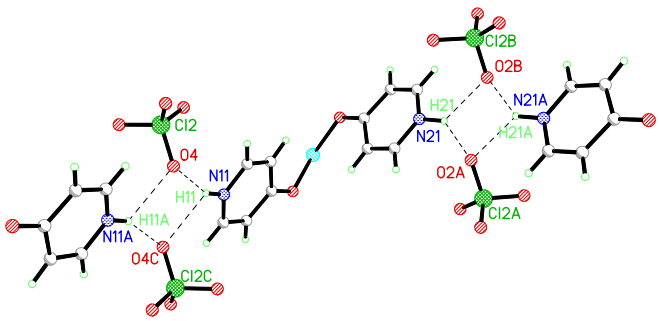

FIG. 4. The bifurcated hydrogen bonds (dashed lines) observed between pyridone ligands and perchlorate ions of CPPP viewed parallel to the body diagonal.

TABLE III. Hydrogen bond lengths (d in Å) and angles ($\angle$ in degrees) for CPPP (here, D is a donor and A is an acceptor). Symmetry transformations used to generate equivalent atoms: #1 $-x+1, -y+1, -z+1$; #2 $-x+1, y-3/2, -z+1/2$; #3 $x, -y+1/2, z-1/2$.

D-H...A	d(D-H)	d(H...A)	d(D...A)	$\angle$(DHA)
N11-H11...O4	0.86(3)	2.14(3)	2.946(3)	155(3)
N11-H11 . . . O4#1	0.86(3)	2.49(3)	3.111(3)	129(3)
N21-H21 . . . O2#2	1.03(3)	2.12(3)	2.975(3)	139(2)
N21-H21 . . . O2#3	1.03(3)	2.24(3)	3.055(3)	135(2)

measurements of single-crystal samples. The data obtained for $H \parallel a^*$ are summarized in Fig. 7, revealing $\mu_0 H_{c1} = 4.63(5)$ T and $\mu_0 H_{c2} = 22.78(5)$ T (measured at 20 mK). With increasing temperature (starting approximately at 400 mK) the phase transitions become less sharp, washed out by thermal fluctuations. Results of the DMRG calculation for zero-temperature magnetization (in the calculations we used $J_{\rm rung}/k_B = 12.1$ K, $J_{\rm leg}/k_B = 10.5$ K, and $g_{a^*} = 2.147$) are shown in Fig. 7 by the dotted line, leading to $\mu_0 H_{c1} = 4.42$ T and $\mu_0 H_{c2} = 22.95$ T. These values are in excellent agreement with the experimentally observed critical fields. Both critical fields shift to higher values, when the applied magnetic field is tilted to the c direction (Fig. 8), so that for $H \parallel c$ we obtained $\mu_0 H_{c1} = 4.80(5)$ T and $\mu_0 H_{c2} = 23.88(5)$ T. Interestingly, recent infrared spectroscopy studies of CPPP [39] showed pronounced changes in the pyrazine-related vibrational phonon spectra across different regions of the phase diagram, revealing a significant role of spin-lattice coupling in this compound.

As mentioned, at H_{c1} the system undergoes a transition into the low-temperature TTL phase. Typically, upon decreasing temperature, 3D interactions become relevant, resulting in a field-induced magnetically ordered ground state. Usually, such a transition can be observed by means of specific-heat measurements (see, e.g., Refs. [19,40–42]). Our thorough search using a heat-capacity technique did not reveal any signature of the field-induced 3D ordering at least down

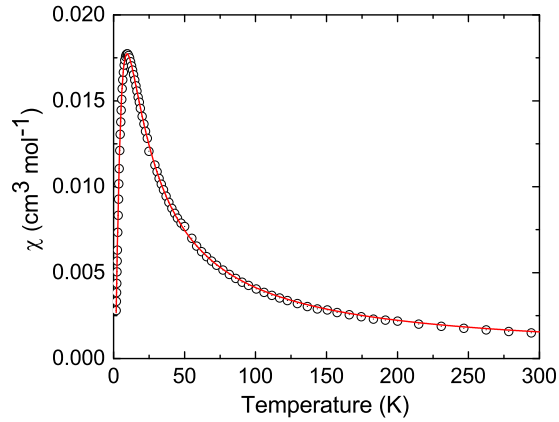

FIG. 5. Magnetic susceptibility of a powder CPPP sample as collected in a 1 kOe field (symbols). Results of calculations are shown by the red line (see text for details).

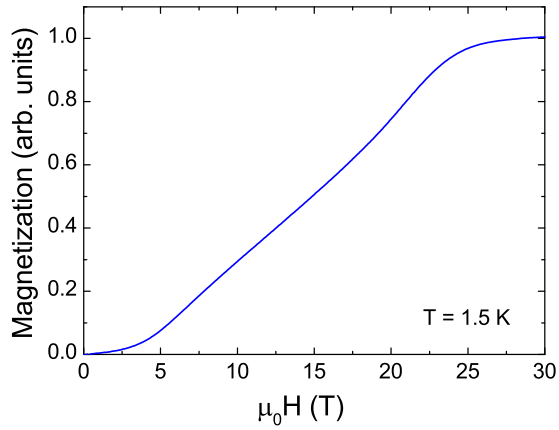

FIG. 6. Pulsed-field magnetization of a powder CPPP sample at a temperature of 1.5 K.

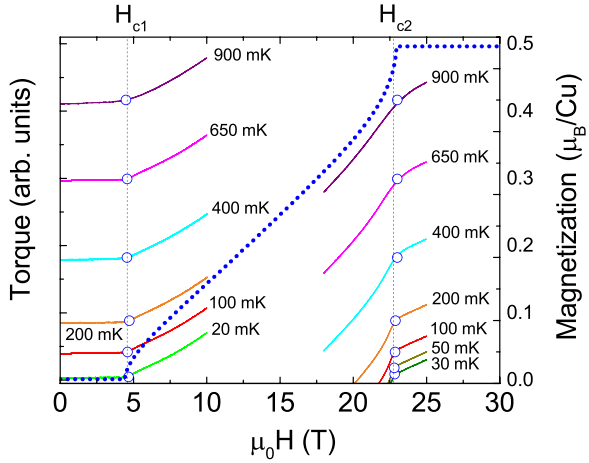

FIG. 7. Temperature dependences of the first and second critical fields, as determined by torque magnetometry (symbols) for $H \parallel a^*$. Examples of torque signals at different temperatures in the vicinity of critical fields are shown by solid lines (the data are offset for clarity, in accordance with the measurement temperature). The calculated zero-temperature magnetization is shown by the blue dotted line (see text for details).

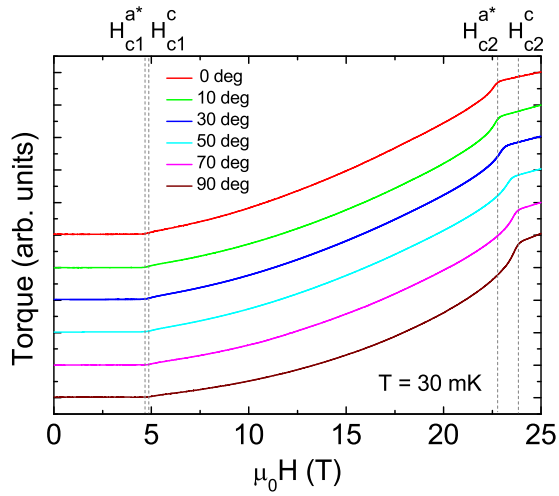

FIG. 8. Angular dependence of the torque signal at a temperature of 30 mK. The angle 0° corresponds to $H \parallel a^*$, while 90° corresponds to $H \parallel c$. The data are rescaled and offset for clarity.

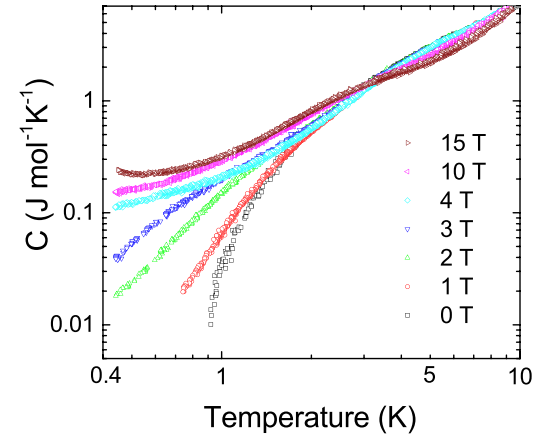

FIG. 9. Specific heat of CPPP measured in magnetic fields up to 15 T ($H \parallel a^*$).

to ∼450 mK (Fig. 9), suggesting a very small interladder coupling J'.

Finally, we would like to comment on some ESR properties of CPPP. Room-temperature ESR on a single crystal revealed $g_{a^*} = 2.147(3)$, $g_b = 2.183(6)$, and $g_c = 2.077(4)$ [$g_{a^*} = 2.147(3)$ was used to calculate the single-crystal magnetization for $H \parallel a^*$ (Fig. 7)]. The temperature dependence of the integrated intensity [Fig. 10(a)] demonstrated a pronounced maximum at about 15 K, a signature of the excited triplet separated from the ground state by a gap [Fig. 10(a) inset].

Upon decreasing temperature below approximately 30 K, the ESR line developed substantial broadening [accompanied by a pronounced shift of the resonance field, Figs. 10(b) and 10(c)], followed by a splitting of the ESR spectrum in two $\Delta M_s = 1$ components (lines A and B in Figs. 11 and 12). Such behavior is a clear indication of the triplet splitting, caused by anisotropic magnetic dipole-dipole coupling [43–45], schematically shown in the inset of Fig. 10(a).

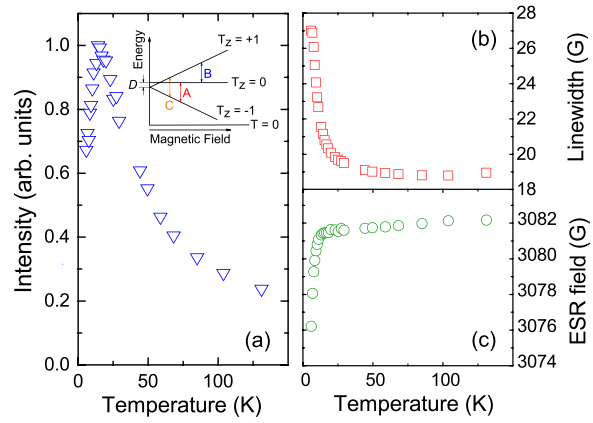

FIG. 10. Temperature dependences of (a) the ESR integrated intensity, (b) linewidth, and (c) magnetic field, measured at a frequency of 9.4 GHz with magnetic field applied parallel to the b axis. The inset shows a schematic view of the low-energy level diagram with the spin-singlet ground state $T = 0$ and first excited triplet split by the small anisotropy term D.

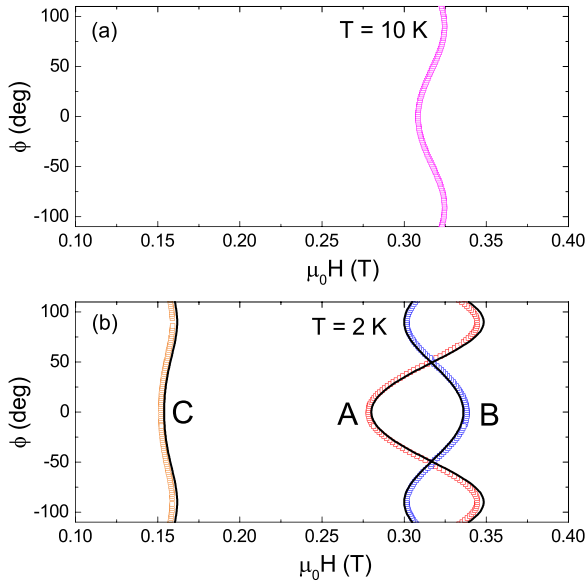

FIG. 11. Angular dependences of the ESR magnetic fields in the *bc* plane measured at a frequency of 9.4 GHz at (a) 10 K and (b) 2 K. ϕ is the angle between the direction of the applied magnetic field and the *b* axis. Fit results are shown by black solid lines.

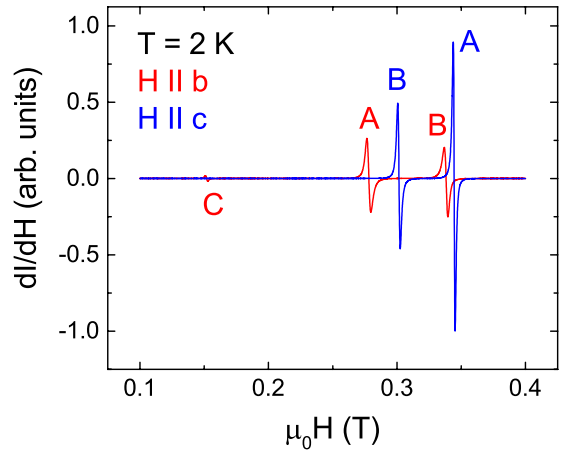

FIG. 12. ESR spectra at 2 K for $H \parallel b$ (red) and $H \parallel c$ (blue). I is the microwave intensity and H is the applied magnetic field; the spectra are collected at a frequency of 9.4 GHz.

Results of the low-temperature ESR simulations with $D = 34$ mK and $E = 16$ mK for the axial and in-plane orthorhombic anisotropy terms, respectively, are shown in Fig. 11(b) by black lines, revealing a tiny crystal-field anisotropy ($\sim$0.4% of $J_{\rm rung}$). The low-field resonance C corresponds to a $\Delta M_s = 2$ transition, which is nominally forbidden, but becomes allowed if wave functions from neighboring spin levels are mixed.

VI. CONCLUSIONS

We reported on the synthesis and extensive magnetic, thermodynamic, and electron-spin-resonance studies of the coordination complex $[Cu_2(pz)_3(HOpy)_4](ClO_4)_4$, which is identified as a quantum spin-1/2 ladder system with the exchange-coupling parameters $J_{\rm rung}/k_B = 12.1(1)$ K and $J_{\rm leg}/k_B = 10.5(3)$ K, and modest critical fields. The coupling parameters, obtained from the analysis of the temperature dependence of magnetic susceptibility, are found in excellent agreement with the results of numerical calculations, performed for the high-field magnetization. The absence of a resolvable field-induced long-range ordering in specific heat down to 0.45 K (indicative of the very good ladder isolation) and the presence of a very small crystal-field anisotropy ($\sim$0.4% of $J_{\rm rung}$) makes $[Cu_2(pz)_3(HOpy)_4](ClO_4)_4$ a very attractive model system to study the physical properties of a quantum spin-1/2 Heisenberg AF ladder close to the isotropic limit.

ACKNOWLEDGMENTS

This work was supported by the Deutsche Forschungsgemeinschaft, through ZV 6/2-2, the Würzburg-Dresden Cluster of Excellence on Complexity and Topology in Quantum Matter - *ct.qmat* (EXC 2147, Project No. 390858490), and SFB 1143, as well as by the HLD at HZDR and LNCMI-CNRS, members of the European Magnetic Field Laboratory (EMFL). This project was supported in part by the Swiss National Science Foundation under Division II We would like to thank A. Ozarowski for providing the access to his ESR simulation program SPIN, and J. Klotz, J.-H. Park, D. Graf, M. Uhlarz, S. Chattopadhyay, and T. Herrmannsdörfer for test measurements of CPPP. We thank C. Kollath for her involvement in the development of the DMRG code used in this study. We acknowledge the discussion with M. Vojta. M.M.T. and C.P.L. are grateful for a National Science Foundation Grant No. (IMR-0314773) for the Quantum Design MPMS magnetometer.

[1] E. Dagotto and T. M. Rice, Science **271**, 618 (1996).
[2] T. Giamarchi, *Quantum Physics in one Dimension*, International Series of Monographs on Physics Vol. 121 (Oxford University Press, Oxford, U.K., 2004).
[3] M. Sigrist, T. M. Rice, and F. C. Zhang, Phys. Rev. B **49**, 12058 (1994).
[4] M. Uehara, T. Nagata, J. Akimitsu, H. Takahashi, N. Môri, and K. Kinoshita, J. Phys. Soc. Jpn. **65**, 2764 (1996).
[5] T. Giamarchi, C. Rüegg, and O. Tchernyshyov, Nat. Phys. **4**, 198 (2008).
[6] V. Zapf, M. Jaime, and C. D. Batista, Rev. Mod. Phys. **86**, 563 (2014).
[7] M. Klanjšek, H. Mayaffre, C. Berthier, M. Horvatić, B. Chiari, O. Piovesana, P. Bouillot, C. Kollath, E. Orignac, R. Citro, and T. Giamarchi, Phys. Rev. Lett. **101**, 137207 (2008).
[8] P. Bouillot, C. Kollath, A. M. Läuchli, M. Zvonarev, B. Thielemann, C. Rüegg, E. Orignac, R. Citro, M. Klanjšek, C.

Berthier, M. Horvatić, and T. Giamarchi, Phys. Rev. B **83**, 054407 (2011).

[9] B. Thielemann, C. Rüegg, H. M. Rønnow, A. M. Läuchli, J.-S. Caux, B. Normand, D. Biner, K. W. Krämer, H.-U. Güdel, J. Stahn, K. Habicht, K. Kiefer, M. Boehm, D. F. McMorrow, and J. Mesot, Phys. Rev. Lett. **102**, 107204 (2009).

[10] T. Barnes, E. Dagotto, J. Riera, and E. S. Swanson, Phys. Rev. B **47**, 3196 (1993).

[11] M. Reigrotzki, H. Tsunetsuugu, and T. M. Rice, J. Phys.: Condens. Matter **6**, 9235 (1994).

[12] M. Greven, R. J. Birgeneau, and U. J. Wiese, Phys. Rev. Lett. **77**, 1865 (1996).

[13] T. Giamarchi and A. M. Tsvelik, Phys. Rev. B **59**, 11398 (1999).

[14] C. P. Landee and M. M. Turnbull, J. Coord. Chem. **67**, 375 (2014).

[15] A. Shapiro, C. P. Landee, M. M. Turnbull, J. Jornet, M. Deumal, J. J. Novoa, M. A. Robb, and W. Lewis, J. Am. Chem. Soc. **129**, 952 (2007).

[16] T. Hong, Y. H. Kim, C. Hotta, Y. Takano, G. Tremelling, M. M. Turnbull, C. P. Landee, H.-J. Kang, N. B. Christensen, K. Lefmann, K. P. Schmidt, G. S. Uhrig, and C. Broholm, Phys. Rev. Lett. **105**, 137207 (2010).

[17] J. L. White, C. Lee, O. Gunaydin-Sen, L. C. Tung, H. M. Christen, Y. J. Wang, M. M. Turnbull, C. P. Landee, R. D. McDonald, S. A. Crooker, J. Singleton, M. H. Whangbo, and J. L. Musfeldt, Phys. Rev. B **81**, 052407 (2010).

[18] D. Schmidiger, S. Mühlbauer, S. N. Gvasaliya, T. Yankova, and A. Zheludev, Phys. Rev. B **84**, 144421 (2011).

[19] D. Schmidiger, P. Bouillot, S. Mühlbauer, S. Gvasaliya, C. Kollath, T. Giamarchi, and A. Zheludev, Phys. Rev. Lett. **108**, 167201 (2012).

[20] M. Jeong, H. Mayaffre, C. Berthier, D. Schmidiger, A. Zheludev, and M. Horvatić, Phys. Rev. Lett. **111**, 106404 (2013).

[21] D. Schmidiger, P. Bouillot, T. Guidi, R. Bewley, C. Kollath, T. Giamarchi, and A. Zheludev, Phys. Rev. Lett. **111**, 107202 (2013).

[22] D. Schmidiger, S. Mühlbauer, A. Zheludev, P. Bouillot, T. Giamarchi, C. Kollath, G. Ehlers, and A. M. Tsvelik, Phys. Rev. B **88**, 094411 (2013).

[23] M. Ozerov, M. Maksymenko, J. Wosnitza, A. Honecker, C. P. Landee, M. M. Turnbull, S. C. Furuya, T. Giamarchi, and S. A. Zvyagin, Phys. Rev. B **92**, 241113(R) (2015).

[24] V. N. Glazkov, M. Fayzullin, Y. Krasnikova, G. Skoblin, D. Schmidiger, S. Mühlbauer, and A. Zheludev, Phys. Rev. B **92**, 184403 (2015).

[25] B. R. Patyal, B. L. Scott, and R. D. Willett, Phys. Rev. B **41**, 1657 (1990).

[26] B. C. Watson, V. N. Kotov, M. W. Meisel, D. W. Hall, G. E. Granroth, W. T. Montfrooij, S. E. Nagler, D. A. Jensen, R. Backov, M. A. Petruska, G. E. Fanucci, and D. R. Talham, Phys. Rev. Lett. **86**, 5168 (2001).

[27] T. Lorenz, O. Heyer, M. Garst, F. Anfuso, A. Rosch, C. Rüegg, and K. W. Krämer, Phys. Rev. Lett. **100**, 067208 (2008); F. Anfuso, M. Garst, A. Rosch, O. Heyer, T. Lorenz, C. Rüegg, and K. W. Krämer, Phys. Rev. B **77**, 235113 (2008).

[28] A. T. Savici, G. E. Granroth, C. L. Broholm, D. M. Pajerowski, C. M. Brown, D. R. Talham, M. W. Meisel, K. P. Schmidt, G. S. Uhrig, and S. E. Nagler, Phys. Rev. B **80**, 094411 (2009).

[29] B. Thielemann, C. Rüegg, K. Kiefer, H. M. Rønnow, B. Normand, P. Bouillot, C. Kollath, E. Orignac, R. Citro, T. Giamarchi, A. M. Läuchli, D. Biner, K. Krämer, F. Wolff-Fabris, V. Zapf, M. Jaime, J. Stahn, N. B. Christensen, B. Grenier, D. F. McMorrow *et al.*, Phys. Rev. B **79**, 020408(R) (2009).

[30] E. Čižmár, M. Ozerov, J. Wosnitza, B. Thielemann, K. W. Krämer, C. Rüegg, O. Piovesana, M. Klanjšek, M. Horvatić, C. Berthier, and S. A. Zvyagin, Phys. Rev. B **82**, 054431 (2010).

[31] J. Jornet-Somoza, N. Codina-Castillo, M. Deumal, F. Mota, J. J. Novoa, R. T. Butcher, M. M. Turnbull, B. Keith, C. P. Landee, and J. L. Wikaira, Inorg. Chem. **51**, 6315 (2012).

[32] M. Deumal, G. Giorgi, M. A. Robb, M. M. Turnbull, C. P. Landee, and J. J. Novoa, Eur. J. Inorg. Chem. **25**, 4697 (2005).

[33] CrysAlisPro, Agilent Technologies, Version 1.171.35.21 (release 20-01-2012 CrysAlis171.NET).

[34] G. M. Sheldrick, Acta Crystallogr., Sect. A **64**, 112 (2008).

[35] G. M. Sheldrick, Acta Crystallogr., Sect. C **71**, 3 (2015).

[36] Y. Skourski, M. D. Kuz'min, K. P. Skokov, A. V. Andreev, and J. Wosnitza, Phys. Rev. B **83**, 214420 (2011).

[37] Y. Wang, T. Plackowski, and A. Junod, Physica C **355**, 179 (2001).

[38] D. C. Johnston, M. Troyer, S. Miyahara, D. Lidsky, K. Ueda, M. Azuma, Z. Hiroi, M. Takano, M. Isobe, Y. Ueda, M. A. Korotin, V. I. Anisimov, A. V. Mahajan, and L. L. Miller, arXiv:cond-mat/0001147.

[39] K. Hughey, N. C. Harms, K. R. O'Neal, A. J. Clune, J. C. Monroe, A. L. Blockmon, C. P. Landee, Z. Liu, M. Ozerov, and J. L. Musfeldt, Inorg. Chem. **59**, 2127 (2020).

[40] A. Oosawa, H. Aruga Katori, and H. Tanaka, Phys. Rev. B **63**, 134416 (2001).

[41] M. Jaime, V. F. Correa, N. Harrison, C. D. Batista, N. Kawashima, Y. Kazuma, G. A. Jorge, R. Stein, I. Heinmaa, S. A. Zvyagin, Y. Sasago, and K. Uchinokura, Phys. Rev. Lett. **93**, 087203 (2004).

[42] Y. Kohama, A. V. Sologubenko, N. R. Dilley, V. S. Zapf, M. Jaime, J. A. Mydosh, A. Paduan-Filho, K. A. Al-Hassanieh, P. Sengupta, S. Gangadharaiah, A. L. Chernyshev, and C. D. Batista, Phys. Rev. Lett. **106**, 037203 (2011).

[43] J. Krzystek, J. U. von Schütz, G. Ahlgren, J. Hellberg, S. Söderholm, and G. Olovsson, J. Phys. (Paris) **47**, 1021 (1986).

[44] J. Krzystek and J. U. von Schütz, in *Advances in Chemical Physics*, edited by I. Prigogine and S. A. Rice (Wiley, New York, 1993), Vol. LXXXVI, pp. 167–329.

[45] S. A. Zvyagin, J. Wosnitza, J. Krzystek, R. Stern, M. Jaime, Y. Sasago, and K. Uchinokura, Phys. Rev. B **73**, 094446 (2006).